

The Kataura plot for single wall carbon nanotubes on top of crystalline quartz

Jaqueline S. Soares^{*1}, Luiz G. Cançado¹, Eduardo B. Barros², and Ado Jorio¹

¹ Departamento de Física, Universidade Federal de Minas Gerais, Belo Horizonte 31270-901, MG, Brazil

² Departamento de Física, Universidade Federal do Ceará, Fortaleza 60455-760, CE, Brazil

Received 30 April 2010, revised 12 July 2010, accepted 15 July 2010

Published online 13 September 2010

Keywords carbon nanotube, Raman spectroscopy, substrate interaction

* Corresponding author: e-mail jssoares@fisica.ufmg.br, Phone: +55 31 3409 6610, Fax: +55 31 3409 5600

In this work, we have studied the radial breathing mode (RBM) resonance Raman spectra of single-wall carbon nanotube serpentines. Each serpentine consists of a series of straight, parallel, and regularly spaced segments, connected by alternating U-turns formed on top of crystalline miscut quartz. We compare our ω_{RBM} and E_{ii} values with the results in the literature and find a strong environmental effect related to the

tube–substrate interaction. We establish experimentally the $\omega_{\text{RBM}} = (227/d_t)\sqrt{1 + (0.082 \pm 0.009)d_t^2}$ relation between RBM frequency (ω_{RBM}) and tube diameter (d_t), with a 100 ± 30 meV downshift in the optical transition energies with respect to the E_{ii} values measured for the standard “super-growth” samples.

© 2010 WILEY-VCH Verlag GmbH & Co. KGaA, Weinheim

1 Introduction The Raman spectroscopy technique has been widely used to characterize single wall carbon nanotubes (SWNTs) and graphene [1]. The mapping technique based on Raman spectroscopy makes it possible to spatially resolve the SWNT related to specific Raman features, such as the radial breathing mode (RBM) and the tangential modes (G-band), thereby facilitating the study of local environmental effects on the Raman features from one single SWNT. For example, effects introduced by SWNTs sitting on substrates have been studied through comparative lineshape analysis of freely suspended SWNTs crossing trenches versus sitting on substrates [2, 3]. The RBM feature corresponds to the coherent vibration of the C atoms in the radial direction, as if the tube was “breathing.” The RBM frequency (ω_{RBM}) can be used to obtain the nanotube diameter (d_t), to probe the electronic structure through its intensity (I_{RBM}) and, consequently, to perform an (n,m) assignment of a single isolated SWNT from the analysis of both d_t and I_{RBM} [4]. It is useful to have the so-called Kataura plot [5] (E_{ii} vs. d_t) on hand when acquiring the RBM spectra from a SWNT sample for making the (n,m) assignments of individual isolated SWNTs.

The (n,m) identification of an individual single-walled carbon nanotube can be significantly affected by the surrounding environment. To ensure the accuracy of the

chirality identification, it is important to find out how various environmental conditions alter the E_{ii} or ω_{RBM} values. There are different results when the SWNT is freely suspended or when it is interacting with the substrate [2, 3]. A class of SWNTs, called “super-growth,” has their ω_{RBM} to d_t relation given by $\omega_{\text{RBM}} = 227/d_t$ [6]. These SWNTs follow a simple linear relation between ω_{RBM} and d_t , in agreement with the elastic properties of graphite [7], and with a negligible environmental effect [6, 8]. All the observed ω_{RBM} values reported in the literature are upshifted from this fundamental relation [8–17]. This upshift was explained based on the van der Waals forces, which mediate the interactions between the tube wall and the surrounding environment [6, 8]. Here we show the experimental efforts made to establish the E_{ii} and ω_{RBM} of carbon nanotubes sitting on crystalline quartz, to guide the (n,m) assignment of such samples.

2 Experimental details Carbon nanotube serpentines were grown by catalytic chemical vapor deposition (CVD) on miscut single-crystal quartz wafers, as previously reported [18]. The resulting vicinal α -SiO₂ (1 $\bar{1}$ 0 1) substrate is insulating, and terminated with parallel atomic steps [18]. Raman spectra were collected at room temperature in air at various points along the SWNT serpentines. Here we use three excitation laser energies: 1.58 eV (785.4 nm), 1.96 eV

© 2010 WILEY-VCH Verlag GmbH & Co. KGaA, Weinheim

(632.8 nm), and 2.33 eV (532 nm). With the excitation energies of 1.58 and 1.96 eV, the Raman spectra were collected using a shamrock sr-303i spectrometer from AndorTM Technology. Confocal Raman measurements were performed on an inverted optical microscope (Nikon – Eclipse TE2000-U) with the addition of an x, y-stage for raster-scanning the sample. For the laser line of 2.33 eV, the Raman spectra were measured on an ALPHA 300 spectrometer from WITEC. Both systems are equipped with charged-coupled device (CCD) detectors.

3 Results and analysis Figure 1a shows the optical transition energies (E_{ii}) for each (n,m) SWNT as a function of the RBM frequency, i.e., the so-called “Kataura plot” for the standard “super-growth” samples. E_{ii} is ranging from E_{11}^S up to E_{66}^S (here S stands for semiconducting tube; while M will be used for metallic tubes). A Raman peak appears at a given ω_{RBM} when resonance is established for a given carbon nanotube in the sample [9]. The data in Fig. 1a use the relation $\omega_{\text{RBM}} = 227/d_t$ [6] and the E_{ii} values were obtained using the equation [8, 19]:

$$E_{ii}(p, d_t) = 1.074 \left(\frac{p}{d_t} \right) \left[1 + 0.467 \log \left(\frac{0.812 d_t}{p} \right) \right] + \frac{\beta_p \cos 3\theta}{d_t^2}, \quad (1)$$

where p is defined as 1, 2, 3, ..., 8 for $E_{11}^S, E_{22}^S, E_{11}^M, \dots, E_{66}^S$, respectively, and the values of β can be found in Refs. [8, 19].

Resonance Raman experiments were performed in the SWNT serpentines. We have measured 38 SWNT serpentines with the three laser lines and found RBMs in 13 cases (up triangles in Fig. 1). With the excitation energy of 1.58 eV, we found seven SWNT serpentines with RBM. In the 1.96 eV laser line we found three SWNT serpentines with RBM and with the excitation energy 2.33 eV we found three SWNT serpentines with RBM. These experimental data have been included in the Kataura plots of Fig. 1 by considering their ω_{RBM} as measured, and resonance condition satisfied by $E_{ii} \approx E_{\text{laser}}$. The (n,m) assignment for the observed RBMs (up triangles in Fig. 1a) cannot be performed using the standard “super-growth” Kataura plot because several up triangles fall in regions where there are no corresponding E_{ii} values from any SWNT (no matching between triangles and circles). Both ω_{RBM} versus d_t relation and the E_{ii} values have to be rescaled due to the substrate interaction.

The E_{ii} data in Fig. 1b stand for the “alcohol-assisted” SWNT samples [9] and use the relation:

$$\omega_{\text{RBM}} = \left(\frac{227}{d_t} \right) \sqrt{1 + C d_t^2} \quad (2)$$

with $C = 0.05786 \text{ nm}^{-2}$ [6]. The optical transition energy values were obtained using Eq. (1), but with different proportionality constants for addressing different samples,

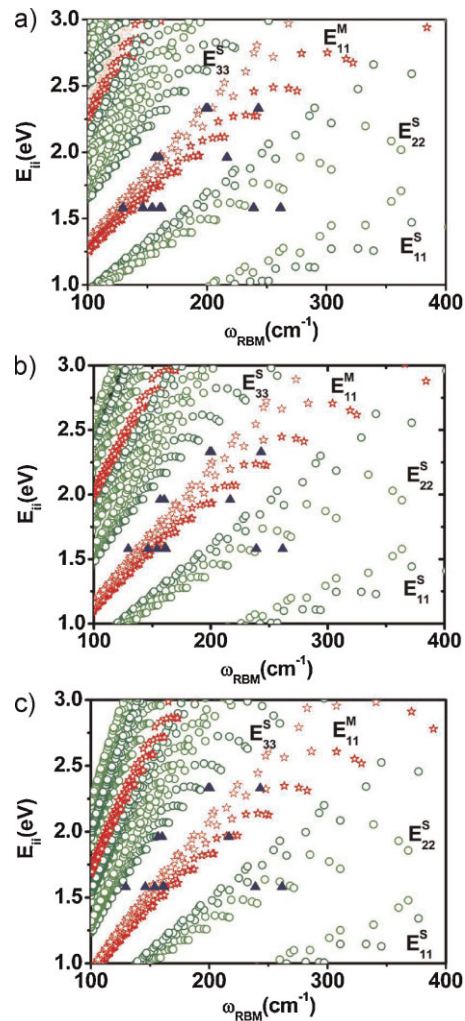


Figure 1 (online colours at: www.pss-b.com) Optical transition energies (E_{ii}) of each (n,m) SWNT plotted versus the respective RBM frequencies, known as the Kataura plot. The optical transition energies of semiconducting (circles) and metallic (stars) SWNTs are shown. Up triangles represent RBM results obtained from resonance Raman spectra, taken from carbon nanotube serpentines. The y-axis coordinate is chosen by considering resonance at $E_{ii} \approx E_{\text{laser}}$. The x-axis is chosen by considering a correspondence between ω_{RBM} and d_t . (a) $\omega_{\text{RBM}} = 227/d_t$ for the “super-growth” standard sample [6], and E_{ii} from Eq. (1); (b) Eq. (2) for ω_{RBM} with $C = 0.05786 \text{ nm}^{-2}$ and E_{ii} for the “alcohol-assisted” SWNTs sample (see text and Refs. [6, 9]); (c) Eq. (2) for ω_{RBM} with $C = 0.082 \text{ nm}^{-2}$ for carbon nanotubes on quartz and a 100 meV downshift in E_{ii} with respect to the standard “super-growth” values.

i.e., 1.049 instead of 1.074 and 0.456 instead of 0.476 [8, 9]. These new values, as well as different β values, were found for the “alcohol-assisted” SWNTs [9], and we use them here because they are representative for several results in the literature [8], with an average downshift of ~ 40 meV with respect to the “super-growth” SWNTs. We see that the (n,m) assignment for the RBMs (up triangles in Fig. 1b) cannot be performed using the “alcohol-assisted” SWNTs either.

The Raman-based (n,m) assignment can be performed using Eq. (2) by properly adjusting the constant C [6] and the optical transition energies. Figure 1c shows the matching between the Kataura plot and all RBM data using Eq. (2) with $C = 0.082 \text{ nm}^{-2}$ and a 100 meV downshift in E_{ii} . Any values in the range $C = 0.082 \pm 0.009 \text{ nm}^{-2}$ and a $100 \pm 30 \text{ meV}$ downshift in E_{ii} give a reasonable fit to the data.

4 Conclusions In summary, we have measured a SWNT-substrate system where the crystalline substrate strongly affects the RBM frequency and resonance energies. For making the (n,m) assignments for the SWNTs on crystalline quartz miscut with the Raman technique, we have two parameters (E_{ii} and C) to adjust in the Kataura plot: (i) The carbon nanotube-substrate exhibits a $\omega_{\text{RBM}}(d_t)$ relation according to Eq. (2), with $C = 0.082 \pm 0.009 \text{ nm}^{-2}$ and (ii) a downshift of $100 \pm 30 \text{ meV}$ in E_{ii} with respect to the standard “super-growth” values [6, 8, 19]. These values cannot be changed arbitrarily because the E_{ii} versus d_t relation is nonlinear.

To understand the effect of the environment on ω_{RBM} and E_{ii} we have compared our results with others available in the literature. The C was found to be 0.05786 nm^{-2} for the “alcohol-assisted” sample [6] and equals to $C = 0.082 \pm 0.009 \text{ nm}^{-2}$ for the SWNT serpentine on crystalline quartz. In general, the ω_{RBM} measured here are higher than all values reported in Ref. [8]. Furthermore, the E_{ii} values for the SWNT serpentines on crystalline quartz measured here are lower than all values published in the literature. These results suggest a stronger interaction between tube and crystalline quartz substrate as compared to other types of samples. This is reasonable, since at tube-growth temperatures, it is expected to have exposed unpassivated Si atoms in the crystalline quartz [20]. In this case, the tube–substrate interaction is expected to exhibit covalent Si–C bonds [21–24].

For the optical transition energies E_{ii} , as predicted by Miyauchi et al. [25], an increase of the dielectric constant of the environment generates a downshift in E_{ii} . The usually obtained results generate a downshift of about $\sim 40 \text{ meV}$ [8]. Again, the shift we observed is stronger. Finally, it has been shown recently that E_{ii} shifts caused by the environment usually depend on d_t and E_{ii} [26]. To perform such a detailed analysis in our samples, resonance Raman experiments are being performed and will be published elsewhere.

Acknowledgements We thank Ernesto Joselevich for the samples and Lukas Novotny for the measurements with the 1.58 eV laser line. J.S.S., E.B.B. and A.J. acknowledge financial support from CNPq, CAPES, Rede Nacional de SPM, Rede Nacional de Pesquisa em Nanotubos de Carbono, and AFOSR/SOARD (award #FA9550-08-1-0236). E.B.B. acknowledges support from the IPDI.

References

- [1] M. S. Dresselhaus, G. Dresselhaus, A. Jorio, A. G. Souza Filho, and R. Saito, *Carbon* **40**, 2043 (2002).
- [2] H. Son, Y. Hori, S. G. Chou, D. Nezich, Ge. G. Samsonidze, G. Dresselhaus, M. S. Dresselhaus, and E. B. Barros, *Appl. Phys. Lett.* **85**, 4744 (2004).
- [3] Y. Zhang, J. Zhang, H. Son, J. Kong, and Z. Liu, *J. Am. Chem. Soc.* **127**, 17156 (2005).
- [4] M. S. Dresselhaus, G. Dresselhaus, R. Saito, and A. Jorio, *Phys. Rep.* **409**, 47 (2005).
- [5] H. Kataura, Y. Kumazawa, Y. Maniwa, I. Umezue, S. Suzuki, Y. Ohtsuka, and Y. Achiba, *Synth. Metals* **103**, 2555 (1999).
- [6] P. T. Araujo, I. O. Maciel, P. B. C. Pesce, M. A. Pimenta, S. K. Doorn, H. Qian, A. Hartschuh, M. Steiner, L. Grigorian, K. Hata, and A. Jorio, *Phys. Rev. B* **77**, 241403(R) (2008).
- [7] G. D. Mahan, *Phys. Rev. B* **65**, 235402 (2002).
- [8] P. T. Araujo, P. B. C. Pesce, M. S. Dresselhaus, K. Sato, R. Saito, and A. Jorio, *Physica E* **42**, 1251 (2010).
- [9] P. T. Araujo, S. K. Doorn, S. Kilina, S. Tretiak, E. Einarsson, S. Maruyama, H. Chacham, M. A. Pimenta, and A. Jorio, *Phys. Rev. Lett.* **98**, 067401 (2007).
- [10] M. Milnera, J. Krti, M. Hulman, and H. Kuzmany, *Phys. Rev. Lett.* **84**, 1324 (2000).
- [11] A. Jorio, R. Saito, J. H. Hafner, C. M. Lieber, M. Hunter, T. McClure, G. Dresselhaus, and M. S. Dresselhaus, *Phys. Rev. Lett.* **86**, 1118 (2001).
- [12] S. M. Bachilo, M. S. Strano, C. Kittrell, R. H. Hauge, R. E. Smalley, and R. B. Weisman, *Science* **298**, 2361 (2002).
- [13] A. Hartschuh, H. N. Pedrosa, L. Novotny, and T. D. Krauss, *Science* **301**, 1354 (2003).
- [14] M. Strano, S. K. Doorn, E. H. Haroz, C. Kittrell, R. H. Hauge, and R. E. Smalley, *Nano Lett.* **3**, 1091 (2003).
- [15] H. Telg, J. Maultzsch, S. Reich, F. Hennrich, and C. Thomsen, *Phys. Rev. Lett.* **93**, 177401 (2004).
- [16] S. K. Doorn, D. A. Heller, P. W. Barone, M. L. Usrey, and M. S. Strano, *Appl. Phys. A* **78**, 1147 (2004).
- [17] M. Paillet, T. Michel, J. C. Meyer, V. N. Popov, L. Henrard, S. Roth, and J. L. Sauvajol, *Phys. Rev. Lett.* **96**, 257401 (2006).
- [18] N. Geblinger, A. Ismach, and E. Joselevich, *Nature Nanotech.* **3**, 195 (2008).
- [19] S. K. Doorn, P. T. Araujo, K. Hata, and A. Jorio, *Phys. Rev. B* **78**, 165408 (2008).
- [20] H. Viehhaus and W. Rossow, *Surf. Sci.* **141**, 341 (1984).
- [21] W. Orellana, R. H. Miwa, and A. Fazzio, *Phys. Rev. Lett.* **91**, 166802 (2003).
- [22] R. H. Miwa, W. Orellana, and A. Fazzio, *Appl. Phys. Lett.* **86**, 213111 (2005).
- [23] S. Berber and A. Oshiyama, *Phys. Rev. Lett.* **96**, 105505 (2006).
- [24] G. W. Peng, A. C. H. Huan, L. Liu, and Y. P. Feng, *Phys. Rev. B* **74**, 235416 (2006).
- [25] Y. Miyauchi, R. Saito, K. Sato, Y. Ohno, S. Iwasaki, T. Mizutani, J. Jiang, and S. Maruyama, *Chem. Phys. Lett.* **442**, 394 (2007).
- [26] P. T. Araujo, A. Jorio, M. S. Dresselhaus, K. Sato, and R. Saito, *Phys. Rev. Lett.* **103**, 146802 (2009).